http://dx.doi.org/10.5935/0103-5053.20130039
J. Braz. Chem. Soc., Vol. 24, No. 2, 304-313, 2013.
Printed in Brazil - ©2013 Sociedade Brasileira de Química
0103 - 5053 $6.00+0.00

Article

Superabsorbent Hydrogel Composite with Minerals Aimed at Water Sustainability

Antônio Sávio G. Magalhães,[a] Manuel P. Almeida Neto,[b]
Maslândia N. Bezerra[c] and Judith P. A. Feitosa*,[c]

[a]*Faculdade de Educação de Itapipoca, Curso de Química, Universidade Estadual do Ceará,*
62500-000 Itapipoca-CE, Brazil

[b]*Instituto Federal de Educação, Ciência e Tecnologia do Rio Grande do Norte (IFRN),*
Campus Caicó, 59300-000 Caicó-RN, Brazil

[c]*Departamento de Química Orgânica e Inorgânica, Universidade Federal do Ceará,*
CP 6021, 60455-760 Fortaleza-CE, Brazil

Hidrogéis superabsorventes à base de acrilamida e acrilato compósito com bentonita ou dolomita foram sintetizados e caracterizados por espectroscopia no infravermelho com transformada de Fourier (FTIR), microscopia eletrônica de varredura (SEM) e difratometria de raios X (XRD). A proporção ideal de acrilamida para acrilato foi determinada em 1:1. A presença de 10% (m/m) de bentonita no hidrogel poli(acrilamida) posteriormente hidrolisado com NaOH aumentou o grau de intumescimento de 1173 para 1270 g água g^{-1} gel. Sendo o acrilato obtido por hidrólise, a lavagem do hidrogel para remoção do excesso de hidróxido mostrou ser um contrassenso considerando o objetivo de economizar água. A constante de velocidade de intumescimento inicial e o tempo para atingir o equilíbrio assim como a capacidade de absorção de água (1058 g água g^{-1} gel) indicam o hidrogel composto do compósito poli(acrilamida-*co*-acrilato de potássio) contendo 10% de dolomita como material potencial para ser utilizado como condicionador de solo. O benefício esperado em termos do uso eficiente de água deverá contribuir para a sustentabilidade da água.

Superabsorbent hydrogels based on an acrylamide/acrylate composite with bentonite or dolomite were synthesized and characterized by Fourier transform infrared (FTIR) spectroscopy, scanning electron microscopy (SEM) and X-ray diffractometry (XRD). The ideal proportion of acrylamide to acrylate was determined as 1:1. The presence of 10% (m/m) bentonite in the polyacrylamide hydrogel further hydrolyzed with NaOH increased the swelling degree from 1173 to 1270 g water g^{-1} gel. Being the acrylate obtained by hydrolysis, the hydrogel washing for removal of the alkali excess showed to be a drawback considering the goal of saving water. The initial swelling rate constant and the time required to reach the equilibrium as well as the water absorption capacity (1058 g water g^{-1} gel) indicate the hydrogel comprised of the poly(acrylamide-*co*-potassium acrylate) composite containing 10% dolomite as a potential material for use as a soil conditioner. The expected benefit in terms of the efficient use of water should contribute to the water sustainability.

Keywords: superabsorbent hydrogel, acrylamide, acrylate, bentonite, dolomite, soil conditioner

Introduction

It is well-known that approximately 77% of the earth surface is covered with water, and of this total, 97.5% (1.351 billion km^3) are saline water and only 2.5% (around 35 million km^3) are freshwater. The water available for anthropogenic use represents less than one third of this, that is ca. 10 million km^3.[1] Physical water scarcity describes a situation in which people do not physically have access to the amount of water and/or water with quality that they need. In 2011, over 1.6 billion people were living in areas of physical water scarcity, which represents 22.9% of the world population.[2] Based on the global population growth, by 2025 nearly 2 billion people will be under the effects of physical water scarcity, i.e., they will have less than 1,000 m^3 of water *per* person *per* year.[3] The areas of

---

*e-mail: judith@dqoi.ufc.br

physical water scarcity will increase and the affected world population will be at least 33%.[4]

Brazil has always been considered a rich country in water and it is estimated that around 12% of the water resources of the world surface are located within its borders. In 2007, the Brazilian *per* capita water availability reached 43,027 m^3 *per* year, well above the world average of 8,209 m^3 *per* capita in the same year. However, this impressive average masks an extremely uneven distribution of water resources among regions. The Amazon River accounts for 75% of the Brazilian freshwater resources but the region comprises only 4% of its population. The Southeast Region, which hosts 73% of the Brazilian population and is the region with the highest agricultural production, accounts for around 10% of the national water resources. However, the most dramatic situation is found in the Northeast Region, which includes most of the semi-arid areas. Accounting for 18% of the Brazilian territory and around 28% of its population, this region has only 5% of the water resources and is subject to recurrent severe droughts, harvest failures and food shortages.[5]

The agriculture in Brazil is an important economic and social sector. In 2010, this sector represented 37,9% of the exports, employed 17,0% of the economically active population and contributed 5,8% to the Brazilian GDP (Gross Domestic Product) (25% considering the agribusiness).[6,7] The country is a very significant global producer of sugarcane, coffee and tropical fruits and an important producer of soy, corn and forest products.[7]

Water and energy are essential resources for food production. In fact, at the global level, 70% of the current freshwater withdrawals are destined for agricultural practices, 11% for municipal use and 19% for consumption by industry.[8] In Brazil, according to the National Water Agency (Agência Nacional de Águas), the percentage of freshwater currently used in agriculture is also 70%, and a huge volume of wastewater is produced. To address the challenges posed by a scarcity of water for food production, it is necessary to conserve water and improve the efficiency of water use and productivity, particularly in arid and semi-arid regions where there is an irregular seasonal rainfall pattern and frequent droughts.[9]

Superabsorbent hydrogels are crosslinked hydrophilic polymers which can absorb huge amounts of water or aqueous solution (more than 100 times their own mass) in a short period of time and consequently swell.[10] Due to this characteristic, they have been used in agriculture and horticulture to retain soil moisture.[11] In fact, they can improve both the water holding and nutrient retention capacity of the soil. In addition, the use of hydrogels can reduce the irrigation frequency and compaction of the soil, inhibit erosion and water runoff and increase the soil aeration and microbial activity.[10] As a result, the cost of agricultural production decreases, the productivity of the soil increases and a more efficient use of water is achieved.[12]

Superabsorbent polymers (SAPs), or hydro-retaining polymers, are used in many countries. In Brazil, they have been applied to soils in which coffee, citric fruits, legumes and vegetables are grown, and in the case of soy, corn and maize crops, the use of SAPs is now being introduced.[13] Also, scientific studies addressing issues such as the effect of SAPs on the production of eucalyptus seedlings,[14,15] on coffee planting,[16] on the survival of *Pinus* and *Araucaria* trees[15] and on sugarcane production have been recently reported.[17]

The SAPs used in agriculture are polyelectrolyte hydrogels often composed of acrylamide, acrylic acid and potassium acrylate.[10] One concern related to these polymers is their toxicity. However, studies have verified that polymers based on acrylamide do not penetrate the skin. The acute toxicity in rats is 4.0 g kg^{-1}. In subchronic doses up to 0.46 g kg^{-1} did not cause negative effects in rats and dogs.[18] Crosslinked polyacrylamides/polyacrylates are even less toxic. Toxicological data for superabsorbents based on sodium acrylate have been reported as follows: acute oral toxicity in rats (LD50) > 5.0 g kg^{-1} and acute skin toxicity in rabbits > 2 g kg^{-1}. Aquatic toxicity toward fish is low, LC50/96 h in *Leuciscus idus* > 5.5 g/L.[19]

The commercial SAPs produced for agriculture are based on pure polymers. However, they are expensive and are not recommended for use in saline water.[20] Recent technological advances included the addition of inorganic materials to form superabsorbent composites.[21-24] In this regard, some clays, such as kaolinite,[25] laponite,[26] montmorillonite,[27] attapulgite,[28] diatomite,[29] vermiculite,[30] alumina[31] and mica,[32] have been added to the polymeric matrix. The presence of minerals improves the mechanical properties, water absorption capacity and biodegradability.[20]

Bentonite and dolomite are abundant and low cost minerals in Brazil. Bentonite is an expandable clay mineral with a typical 2:1 layered structure and belongs to the class of smectites with a unit cell,[33] one example being $0.33M^+ (Al_{1.67}Mg_{0.33})Si_4O_{10}(OH)_2$ (Figure 1a). Dolomite is a mineral, but it is not classified as a clay. It belongs to the class of carbonaceous minerals, dolomite and calcite being the most frequently occurring carbonates.[34] These minerals are not generally present in rocks as isolated minerals but instead are found together as the main carbonates. Calcite is calcium carbonate ($CaCO_3$) and dolomite is calcium and magnesium carbonate [$(CaMg(CO_3)_2$] (Figure 1b).[35]

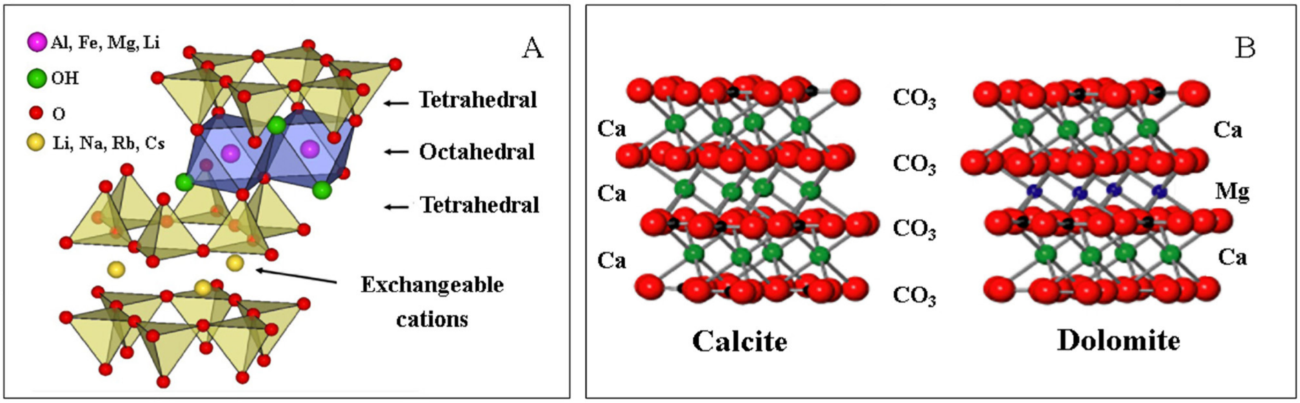

Figure 1. Structure of minerals: smectite-type clay (a), calcite and dolomite (b), adapted from references 35.

Considering all of these factors, superabsorbent hydrogels based on polyacrylamide and minerals (bentonite and dolomite) were synthesized and characterized in order to find the best SAP for use as a soil conditioner, aiming to achieve a more efficient use of water.

Experimental

Materials

Acrylamide (Am), acrylic acid, potassium persulfate (KPS) and *N*,*N*,*N*´,*N*´-tetramethylethylenediamine (TEMED) were obtained from Merck. *N*,*N*'-Methylene bisacrylamide (MBA) was purchased from Sigma Aldrich. Sodium (NaAc) and potassium acrylate (KAc) were prepared by neutralization of acrylic acid with NaOH and KOH, respectively, at up to pH 7.0 in an ice bath. Bentonite was purchased from Bentonisa do Nordeste S.A. (João Pessoa-PB, Brazil) and dolomite from Kimberlit Agrociências Ltda. (Olímpia-SP, Brazil). The commercial hydrogel was donated by Kimberlit Agrociências Ltda. All materials were used as received. Distilled water was used in all experiments.

Characterization of the minerals

The chemical analysis of bentonite was performed by X-ray fluorescence on a Rigaku (ZSX Mini II) fluorometer. The elemental analysis of the dolomite was performed using an inductively coupled plasma/optical emission spectrometer (ICP-AES) with axial views (Optima 4300 Series, Perkin Elmer, USA). Approximately 200 mg of dolomite were transferred to a vial with 5.0 mL of a mixture of HNO_3 (68% m/m) and HCl (37%) in a proportion of 3:1 (v/v). The system was maintained for 10 h. The mixture was heated to 120 °C and held at this temperature for 3 h. It was then cooled, 2 mL of HF (48-51%) were added and the mixture was heated again to 120 °C and held at this temperature for further 3 h. After digestion, all samples were diluted with Milli-Q® water in 25.0 mL volumetric flasks. The blank solution was prepared using the same reagents and procedures, but in the absence of minerals.

Synthesis of hydrogel with acrylamide and sodium acrylate

The hydrogels were synthesized by free-radical copolymerization following the method of Jeon *et al.*[36] and Okay *et al.*[37] with the minor modifications described by Magalhães *et al.*[38] The amounts of MBA, KPS and TEMED were kept constant at 0.5, 0.1 and 0.1 mol%, respectively, based on the total quantity of monomer. The hydrogels were prepared with molar ratios of Am to NaAc varying from 0/100 to 100/0 following the procedure briefly described herein. Acrylamide (freshly-prepared aqueous solution), MBA and KPS were added to an appropriate volume of aqueous sodium acrylate under stirring until complete dissolution of the species. The volume was increased to 50 mL with distilled water, nitrogen was bubbled through the mixture and TEMED was added. The system was kept under further stirring until it reached the gel point. After 24 h, the hydrogel was left to rest, the material was grated, washed and dried in an oven at 60-70 °C, then, it was sieved in order to obtain samples with particle sizes in the range of 100 to 240 µm.

Synthesis of hydrogels with acrylamide and bentonite hydrolyzed with NaOH

Hydrogels with and without bentonite were synthesized applying procedures similar to those previously reported,[38] with some modifications. The amounts of MBA and KPS, that were 0.2 and 0.2 mol%, respectively, differed from those previously used, but the amount of TEMED was the same (0.1 mol%), all values being based on the total quantity of monomer. The other difference is that only acrylamide was employed as monomer. The copolymer was prepared by partial hydrolysis with alkali, which leads to a certain amount of sodium acrylate being present in the polymeric chain.[39] To obtain the hydrogel containing a mineral, the bentonite was first exfoliated by stirring the aqueous suspension for 24 h at ambient temperature.[40] The reaction then proceeded as described for the hydrogel without the mineral. The materials were grated, washed and dried in an oven at 60-70 °C. The dried hydrogels, with and without bentonite, were hydrolyzed with the addition of 0.5 mol L^{-1} NaOH for 3 h at 50 °C. The samples were then washed and sieved in order to obtain particles in the range of 500 to 710 µm. The commercial hydrogel was sieved to obtain the same particle size range.

Synthesis of hydrogels with acrylamide and potassium acrylate composite with dolomite

Hydrogels with and without dolomite were synthesized applying the procedure described for the hydrogel without mineral,[38] with some modifications. The amounts of MBA, KPS and TEMED, as in the case of bentonite addition, were 0.2, 0.2 and 0.1 mol%, respectively. To avoid the need of washing to remove the NaOH excess (used for the hydrolysis), as described in the previous section, and also to guarantee the proportions of acrylamide and acrylate in the copolymer, the monomers were added directly. Taking into account that sodium, in general, has a negative effect on plant growth, and potassium is an important nutrient, potassium acrylate was used. For comparison purposes, hydrogels with and without the mineral were synthesized. The aqueous suspension of dolomite was stirred for 24 h in order to disaggregate the material. The hydrogel was washed and sieved in order to obtain samples with particle sizes in the range of 500 to 710 µm.

The acronyms for the synthesized samples are given in Table 1 and will be used throughout the following section.

Infrared spectroscopic studies

The Fourier transform infrared (FTIR) spectra for the dried hydrogels were recorded with a Shimadzu IR spectrophotometer (model 8300) in the range of 400 to 4000 cm^{-1} as KBr pellets.

Elemental microanalysis

The contents of nitrogen, carbon and hydrogen were determined by elemental microanalysis using a Perkin-Elmer CHN 2400 analyzer.

Degree of swelling

A known mass of hydrogel in the range of 10-50 mg was placed inside a pre-weighed sintered glass filter (No. 0) and covered with distilled water at room temperature (25 ± 1 °C) until the swelling equilibrium was reached. The glass filter was then removed from the water, and the water excess was drained by gravity for a few minutes. The external and internal container walls that were not in contact with the hydrogel were dried and the system was re-weighed.

The equilibrium degree of swelling (W_{eq}) was determined by the equation 1:

$$W_{eq} = \frac{m_{sw} - m_{dr}}{m_{dr}} \quad (1)$$

where m_{sw} and m_{dr} are the masses of swollen and dry polymer, respectively. All swelling experiments were repeated at least three times.

The swelling kinetics was determined in a similar way. The sintered glass filter containing hydrogels were immersed in distilled water and removed for weighing initially at intervals of 10 s and subsequently at longer intervals. After weighing, the hydrogels were returned

Table 1. Acronyms used for the synthesized hydrogels based on acrylamide and acrylate

Acronym	Monomer A	Monomer B	Mineral	MBA / mol%	Reaction after gelation
Am/NaAc	acrylamide	sodium acrylate	–	0.5	–
Pam	acrylamide	–	–	0.2	–
PamH	acrylamide	–	–	0.2	hydrolysis with NaOH
Pam/Bent	acrylamide	–	bentonite	0.2	–
PamH/Bent	acrylamide	–	bentonite	0.2	hydrolysis with NaOH
Pam/Ac	acrylamide	potassium acrylate	–	0.2	–
Pam/Ac/Dol	acrylamide	potassium acrylate	dolomite	0.2	–

MBA: *N,N'*-methylene bisacrylamide.

to their original container. The kinetic experiments were carried out in duplicate.

X-ray diffraction (XRD) analysis

The X-ray powder diffraction (XRD) of different dried hydrogels was carried out in a Rigaku diffractometer (model DMAXB) with Cu K_α radiation, with 2θ varying from 5 to 70°. Prior to the analysis, the materials were sieved and only the particles which passed through a 325 mesh (< 44 µm) sieve were subject to analysis.

Scanning electron microscopy (SEM)

Surface images of the hydrogels were acquired on a Phillips XL 30 scanning electron microscope. The hydrogels were left to swell in water until equilibrium, cut into small slices, freeze dried with liquid nitrogen and coated with gold prior to the morphological analysis.

Results and Discussion

Characterization of the minerals

The results for the chemical analysis of bentonite are presented as the percentage of oxides in Table 2. However, the metals in the structure of bentonite (Figure 1a) are not present as oxides but they are represented as the percentage of oxides because this parameter is used as a standard in the analyses. The data show that the proportion of silicon oxide to aluminum oxide was 2:1, which is characteristic of smectites. Based on these data, the chemical composition of the bentonite was $(Na_{0.11}Ca_{0.04})(Al_{0.80}Mg_{0.42}Fe_{0.78})_2Si_4O_{10}(OH)_2$. The relation between Na^+ and Ca^{2+} ions was 2.8:1.0, indicating a sodium-type clay. Kaolinite and quartz were present as minor components, as determined by XRD analysis. The interlayer distance was 1.26 nm, characteristic of sodium bentonite.[41]

Table 2. Chemical species present in bentonite

Species	Al_2O_3	SiO_2	Fe_2O_3	MgO	CaO	K_2O	Na_2O
Amount / %	26.0	59.6	4.5	2.8	1.2	2.6	3.3

The X'Pert HighScore Plus of the PANalytical software applied to the XRD analysis showed that dolomite was composed of two crystalline phases, dolomite and calcite (Figure 2). The calcium and magnesium contents were 8,177 and 2,997 ppm, respectively. The carbonaceous mineral was composed of 73.7% (m/m) dolomite and 26.3% calcite.

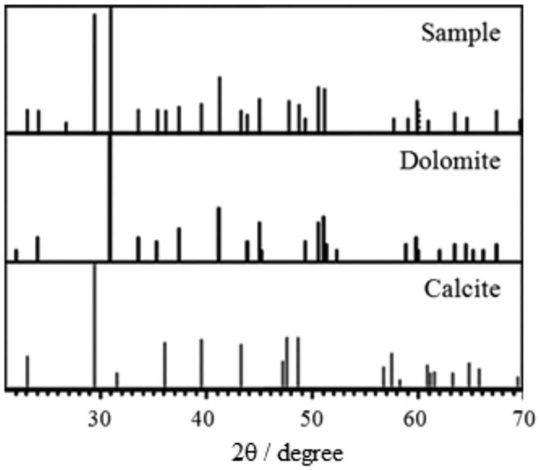

Figure 2. Identification of the crystalline phases in the dolomite sample.

Hydrogels with acrylamide and sodium acrylate

In the case of the hydrogels of poly(acrylamide-*co*-sodium acrylate) crosslinked with 0.5 mol% MBA, the swelling at equilibrium varied according to the percentage of NaAc.[38] Another important factor is how fast the material absorbs water in the first few minutes, in other words, the initial swelling rate constant. Yao and Zhou[42] rewrote the first-order kinetics equation of the Voigt-based model for swelling as:

$$W_t = W_{eq}(1 - e^{-kt}) \tag{2}$$

where W_t and k are the swelling at time t and initial swelling rate constant, respectively.

The degree of swelling at equilibrium and the initial swelling rate constant was determined from a plot of $\ln[W_{eq}/(W_{eq} - W_t)]$ *vs.* t, as reported by Ray and Okamoto.[43] The results are presented in Figure 3. An ideal hydrogel has high W_{eq} and high k values. There was a substantial increase in W_{eq} when the NaAc percentage was higher than 60 and a considerable decrease in the swelling rate constant when the NaAc percentage was higher than 45. Thus, the ideal content of sodium acrylate lies between 45 and 60 mol%. A similar finding was been previously reported for mole fractions of acrylamide ranging from 0.4 to 0.6.[44] An equal proportion of acrylamide and sodium acrylate was thus assumed to be the ideal condition. Under this condition, the W_{eq} value was 172 g water g^{-1} gel. Despite the W_{eq} of the Am/NaAc hydrogel being higher than 100 g water g^{-1} gel (superabsorbent), W_{eq} values higher than 1,000 g water g^{-1} gel have been reported.[10] The content of MBA must be less than 0.5 mol% to improve the swelling of poly(acrylamide-*co*-sodium acrylate). A content of 0.2 mol% was thus tested.

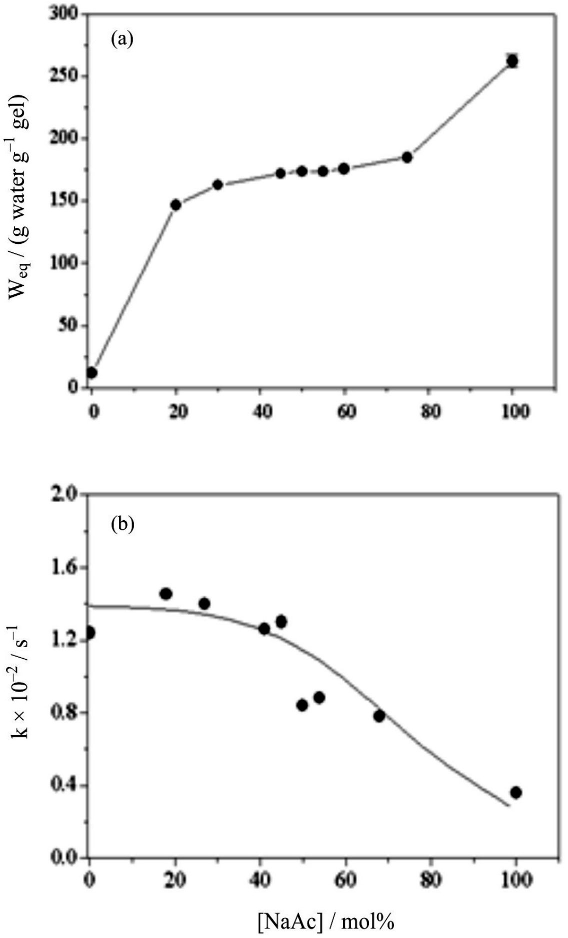

Figure 3. Effect of the sodium acrylate percentage on the swelling equilibrium and the initial swelling rate for hydrogels of poly(acrylamide-*co*-sodium acrylate) crosslinked with 0.5% MBA.

Hydrogels with acrylamide and bentonite hydrolyzed with NaOH

Besides the MBA content, two new parameters were included: the addition of a clay mineral (bentonite) and the obtainment of acrylate from the alkaline hydrolysis of amide groups. The aim was to synthesize hydrogels with an equal proportion of acrylate and acrylamide, assumed to be the ideal condition as described above. For comparison purposes, a hydrogel without the mineral was prepared in the same way. The FTIR bands at 3436, 1041, 523 and 459 cm^{-1} are attributed to ν O–H, ν Si–O, δ Si–O–Al and δ Si–O-Mg of bentonite, respectively (Figure 4A, curve c).[45] The presence of bands at 1568-1570 cm^{-1} and 1403-1404 cm^{-1} is due to ν COO^- of acrylate and confirms the hydrolysis of acrylamide (PamH, PamH/Bent). The bands at 3446 cm^{-1} (ν_{as} NH_2), 3185-3194 cm^{-1} (ν_s NH_2) and 1659-1668 cm^{-1} (ν C=O) are characteristic of the acrylamide unit (Figure 4A, curves a and b). The formation of the composite with bentonite was confirmed by the presence of bands at 1043, 522 and 464 cm^{-1}, attributed to the clay.

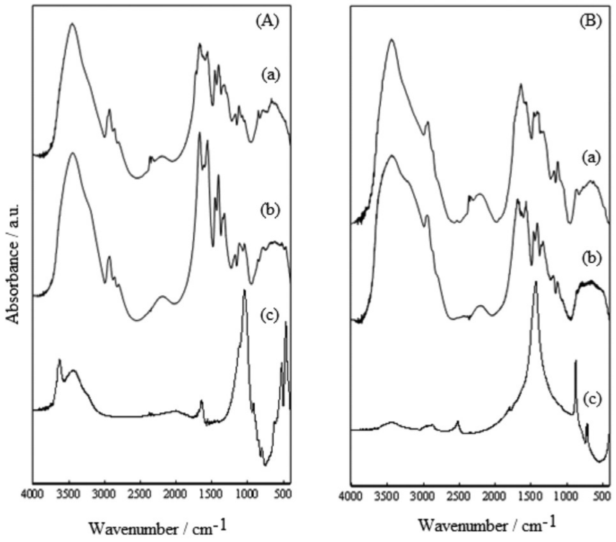

Figure 4. FTIR spectra of hydrogels crosslinked with 0.2 mol% MBA in which (A) shows PamH/Bent (a), PamH (b) and bentonite mineral (c), and (B) shows Pam-Ac/Dol (a), Pam-Ac (b) and dolomite mineral (c).

The molar ratios of acrylamide/acrylate were determined by elemental analysis and also by FTIR spectroscopy, using the relative absorbance of bands at 1410 and 2940 cm^{-1} as proposed by Magalhães *et al.*[38] The Am/NaAc ratios calculated according to the two methodologies were similar (Table 3). However, the PamH and PamH/Bent hydrogels showed different ratios (0.75 ± 0.02 and 0.99 ± 0.01, respectively). The presence of the clay probably leads to a more exposed chain, which makes the hydrolysis with NaOH more efficient.

Table 3. Acrylamide/acrylate molar ratios and chemical analyses of hydrogels synthesized from acrylamide with bentonite before and after alkaline hydrolysis

Hydrogel	C / %	H / %	N / %	Am/NaAc	
				Elemental analysis	FTIR
Pam	42.01	6.82	15.99	–	–
PamH	30.32	4.11	5.11	0.77	0.72
Pam/Bent	42.05	6.60	16.15	–	–
PamH/Bent	32.99	4.57	6.36	0.98	1.00

The XRD pattern of bentonite shows a peak at 2θ at 7.02° (M_{001}), which corresponds to a basal interlayer distance of 1.26 nm (Figure 5A, curve c). In the hydrogel Pam/Bent, the M_{001} is shifted to 2θ at 5.56, with an interlayer distance of 1.63 nm (Figure 5A, curve b). An increase in the distance between the layers is characteristic of an intercalated nanocomposite with polyacrylamide molecules occupying the interlayer space.[46] Also, some degree of crystallinity remains, an indicative of the presence of a microcomposite. A different pattern was found for PamH/Bent (Figure 5A, curve a) in which the absence of peaks suggests the formation of an exfoliated nanocomposite. The hydrolysis after the gelation changed the structure of the material. The ionic charges of the carboxylate group due to the hydrolysis of adsorbed polyacrylamide may repulse each other, leading to a more dispersed clay in the polymeric matrix.

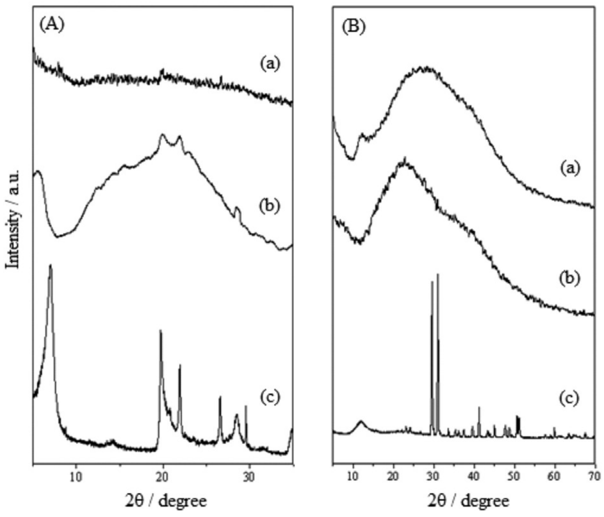

Figure 5. X-ray diffraction patterns for (A): PamH/Bent (a), Pam/Bent (b) and bentonite (c), and for (B): Pam-Ac/Dol (a), Pam-Ac (b) and dolomite (c).

The SEM micrographs showing the hydrogel morphologies can be seen in Figure 6. The Pam/Bent hydrogel shows a compact structure with the presence of clay particles in the range of 2.4-17.9 µm (Figure 6a), in agreement with the formation of a microcomposite, as suggested by the XRD results. In the PamH/Bent hydrogel, a foliated porous structure is apparent, which is very different from that of the unhydrolyzed hydrogel. A similar foliated structure was observed in the micrograph for the PamH hydrogel (image not shown).

In the next synthesis procedure, the concentration of MBA was maintained at 0.2 mol% and equal proportions of acrylate and acrylamide were again used. Since the sodium cation has a negative effect in agricultural practices and potassium is essential, potassium acrylate was used instead of sodium acrylate.

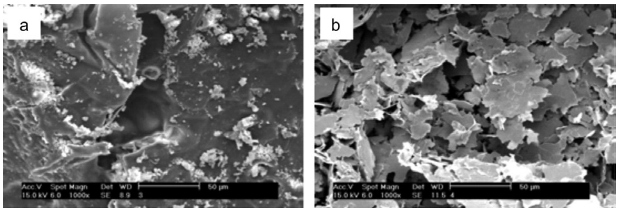

Figure 6. SEM images for Pam/Bent (a) and PamH/Bent (b).

Hydrogels with acrylamide and potassium acrylate composite with dolomite

In case of these hydrogel samples, the addition of a carbonaceous mineral instead of a clay mineral was studied. The molar ratios of acrylamide/acrylate were determined by elemental analysis and were 0.96 and 1.2 for Pam-Ac and Pam-Ac/Dol, respectively. The higher value observed for the hydrogel with dolomite indicates that not all of the acrylate added was copolymerized. This may be due to the interaction of this ionic group with the Ca^{2+} and Mg^{2+} ions in the mineral dispersion and, consequently, a reduction in the availability of the acrylate groups for the copolymerization.

The FTIR spectra for the Pam-Ac and Pam-Ac/Dol hydrogels and the dolomite are shown in Figure 4B. The mineral presented characteristic bands at 1439, 878 and 719 cm^{-1} assigned to the ν_{as} CO_3^{2-}, δ out of plane CO_3^{2-} and δ in plane CO_3^{2-} (Figure 4B, curve c), respectively.[47] The Pam-Ac hydrogels showed bands associated with amide and carboxylate, as discussed in the previous section. Higher absorbance ratios were observed for the C=O band of acrylate (1558 cm^{-1}) and C=O band of amide (1676 cm^{-1}) for Pam-Ac in relation to Pam-Ac/Dol, which is in agreement with the elemental analysis data (Figures 4B, curves a and b). The slight increase in the intensity of the band at 1452 cm^{-1} for the hydrogel with mineral added may be due to the contribution of the ν_{as} CO_3^{2-} band shifted from 1439 cm^{-1}.

The XRD pattern for calcite and dolomite is shown in Figure 5B, curve c. Only an amorphous halo is present in the case of the Pam-Ac hydrogel, as there is no crystallinity (Figure 5B, curve b). No peak from carbonaceous dolomite is observed for the Pam-Ac/Dol hydrogel (Figure 5B, curve a). Thus, the 10% (m/m) of mineral added must be well dispersed in the polymeric matrix. In this case, there are no layers to intercalate the polymer, as occurs with bentonite.

A porous material with an interlaced structure was revealed by the SEM analysis of the hydrogel without dolomite (Figures 7a and 7b). A fibrous morphology is apparent with the inclusion of the mineral in the polymeric matrix (Figures 7c and 7d). The heterogeneous size distribution of the dolomite crystals can be observed (Figures 6e and 6f). Crystals of around 2 µm, and as large as 30 µm, were observed in this sample. A few crystals were

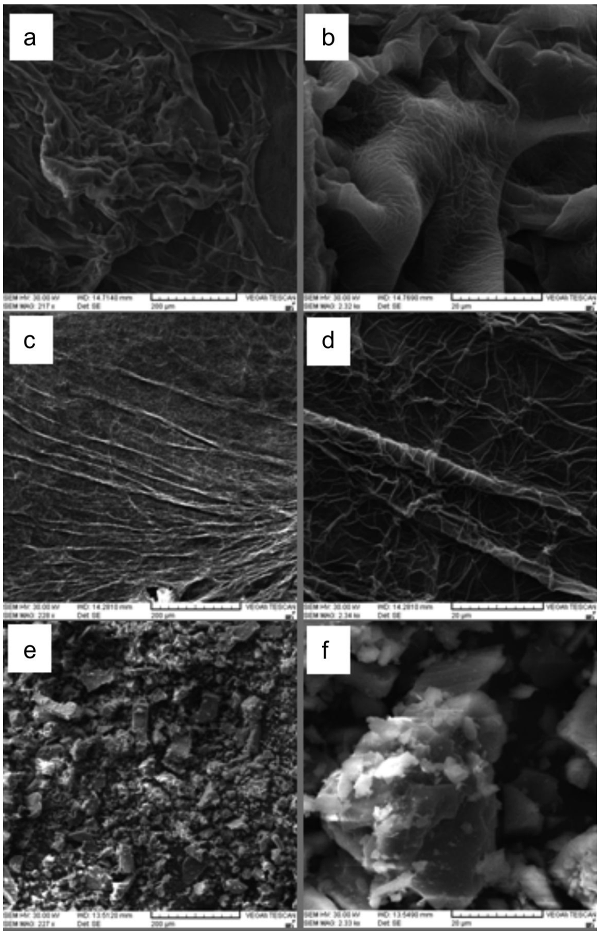

Figure 7. SEM images for Pam-Ac (curves a and b), Pam-Ac/Dol (curves c and d) and dolomite mineral (curves e and f). Scale at 200 µm (curves a, c and e) and scale at 20 µm (curves b, d and f).

present in the image of the Pam-Ac/Dol hydrogel, but not in the same proportion as the mineral added. Most of the dolomite is well dispersed in the copolymer, as indicated by the XRD pattern.

Comparison of swelling characteristics

The swelling curves are shown in Figure 8. For comparison purposes, a commercial hydrogel was also studied. The swelling of all of the hydrogels in water adhered to the well-known behavior, with the water absorption being initially rapid and reaching an equilibrium plateau within a few hours of immersion. The equilibrium swelling values for the hydrogels Pam/Bent, PamH and PamH/Bent were 38 ± 2, 1173 ± 31 and 1270 ± 11 g water g^{-1} gel, respectively. The W_{eq} values increased by factors in the range of 33-36 due to the hydrolysis, which is in agreement with their more foliate and porous structures. The PamH and PamH/Bent hydrogels behaved as superabsorbents, and their W_{eq} values were higher than that obtained for the commercial hydrogel (445 ± 7 g water g^{-1} gel). The major drawback associated with systems that employ hydrolysis is the washing step required to remove the NaOH excess since a large volume of water has to be employed. This is not compatible with the goal of promoting water sustainability.

The kinetics curves for the swelling of the Pam-Ac hydrogel in the presence and absence of dolomite are similar to those previously discussed (Figure 8). The W_{eq} values were 1058 ± 36 and 713 ± 8 g water g^{-1} gel for the Pam-Ac/Dol and Pam-Ac hydrogels, respectively. There are no previously reported data available for hydrogels containing dolomite for comparison purposes.

Besides W_{eq}, two other swelling parameters are important: the initial swelling rate constant (*k*) and the time required to achieve equilibrium (t_{eq}). A comparison of the synthesized hydrogels is provided in Table 4, together with data on the commercial superabsorbent. The commercial hydrogel presented the highest *k* value and the

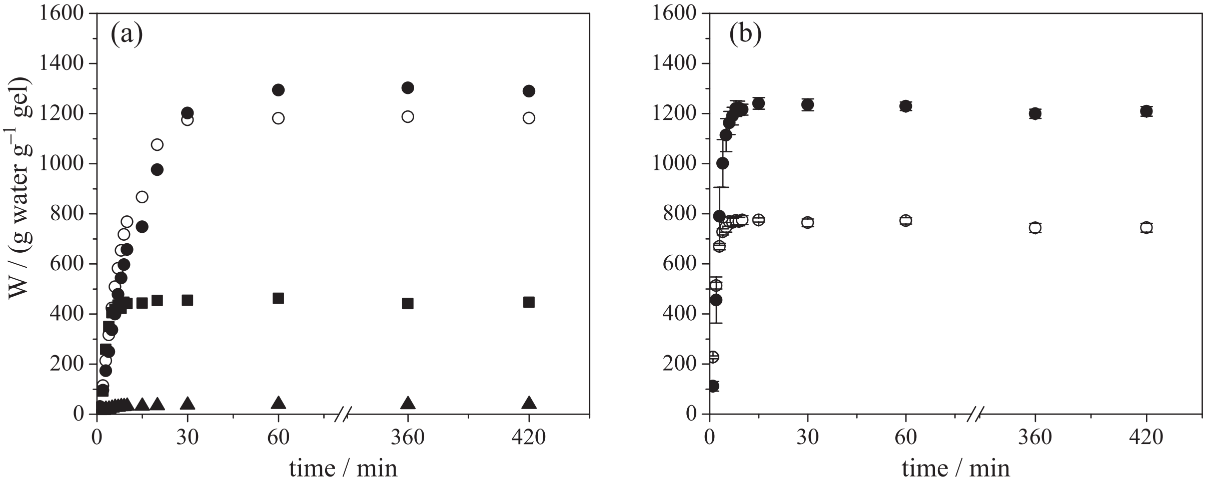

Figure 8. Kinetics of swelling in water for hydrogel samples (a): PamH/Bent (●), Pam/Bent (■), and PamH (○) and a commercial hydrogel (▲), and for (b): Pam-Ac/Dol (●) and Pam-Ac (○).

Table 4. Comparison between different hydrogels produced from acrylamide and acrylate and a commercial superabsorbent

Hydrogel	Cation	Acrylate / mol%	W_{eq} / (g water g^{-1} gel)	t_{eq} / min	*k* / min^{-1}
Pam	–	0	32 ± 4	32	0.096
PamH	Na^+	43	1173 ± 31	43	0.108
Pam/Bent	–	0	38 ± 2	37	0.193
PamH/Bent	Na^+	50	1270 ± 11	86	0.068
Pam-Ac	K^+	51	713 ± 8	22	0.423
Pam-Ac/Dol	K^+	45	1058 ± 36	31	0.370
Commercial	N.I.	N.I.	445 ± 7	15	0.630

N,*N*'-methylene bisacrylamide (MBA): 0.2 mol%; N.I.: not informed.

lowest t_{eq} value but the lowest degree of swelling. From the synthesized materials, PamH/Bent showed the highest W_{eq} value, but the initial swelling rate constant for this sample was the lowest and a very long time was required to reach equilibrium. Besides these negative parameters, the hydrolyzed hydrogels (PamH and PamH/Bent) have to be extensively washed to remove the NaOH added. The Pam-Ac/Dol sample rapidly absorbed a large volume of water, and within 31 min achieved 1058 g water g^{-1} gel.

Conclusions

Superabsorbent hydrogels are easily synthesized by solution copolymerization of acrylamide and acrylate with MBA as a crosslinker agent. The best conditions are equal molar proportions of acrylamide and acrylate and 0.2 mol% of MBA. The addition of minerals (10% of bentonite or dolomite) increases the swelling at equilibrium. Copolymerization using acrylamide and acrylate as monomers is better than polymerization with acrylamide followed by hydrolysis with alkali to transform the amide into a carboxylate group. After these reactions, the alkali excess must be removed from the hydrogel, which requires a substantial amount of water, conflicting with the proposed goal of contributing to water sustainability. The addition of dolomite promotes an increase in the degree of swelling in comparison with the hydrogel without the mineral. The initial swelling rate constant and the time required to reach equilibrium, as well as the water absorption capacity, indicate that hydrogels produced from a poly(acrylamide-*co*-potassium acrylate) composite with dolomite represent potential materials for use in agriculture as a soil conditioner. The consequent increased efficiency in the use of water is expected to contribute to water sustainability.

Acknowledgements

The authors acknowledge financial support from INCT-INOMAT, CT-Hidro, (Conselho Nacional de Desenvolvimento Científico e Tecnológico) (CNPq) and Coordenação de Aperfeiçoamento de Pessoal de Nível Superior (CAPES). The authors also wish to thank Prof. José Marcos Sasaki for recording the X-ray diffractograms. A special acknowledgement is also extended to Prof. Fernando Galembeck for his suggestions, criticisms and friendship, and for drawing attention to the importance of innovation.

References

1. Salati, E.; *Plurale em Revista.* **2011**, *22*, 8, http://www.plurale.com.br/revista-digital.php accessed in January 2013.
2. Boelee, E.; *Ecosystems for Water and Food Security*; United Nations Environment Programme (UNEP) and International Water Management Institute (IWMI): Colombo, Sri Lanka, 2011
3. Rockström, J.; Falkenmark, M.; Karlberg, L.; Hoff, H.; Rost, S.; Gerten, D.; *Water Resour. Res.* **2009**, *44*, W00A12.
4. Rosengrant, M. W.; Cai, X.; Cline, S. A.; *Global Water Outlook to 2025 - Averting an Impending Crisis*; International Food Policy Research Institute: Washington, DC, USA, 2002.
5. Johnson, R. M. F.; Kemper, K. E.; *The World Bank Policy Research Working Paper*; 2005, http://www-wds.worldbank.org/external/default/WDSContentServer/IW3P/IB/ 2005/06/16/000016406_20050616092016/Rendered/PDF/wps3650.pdf.
6. Ministério de Agricultura, http://www.agricultura.gov.br/internacional/indicadores-e-estatisticas/balanca-comercial accessed in June 2012.
7. http://www.dieese.org.br/anu/anuarioRural/ anuarioRural10-11.pdf, accessed in February, 2013.
8. Aquastat, FAO, 2011, www.fao.org/nr/water/aquastat/water_use/index.stm accessed in January 2013.
9. McCartney, M.; Rebelo, L.-M.; Senaratna Sellamuttu, S.; de Silva, S.; *Wetlands, Agriculture and Poverty Reduction*; International Water Management Institute (IWMI Research Report 137): Colombo, Sri Lanka, 2010.
10. Zohuriaan-Mehr, M. J.; Kabiri, K.; *Iran. Polym. J.* **2008**, *17*, 451.

11. Omidian, H.; Rocca, J. G.; Park, K.; *J. Controlled Release* **2005**, *102*, 279.
12. Du, C.; Tang, D.; Zhou, J.; Wang, A.; Shaviv, A.; *Biosystems Eng.* **2008**, *99*, 478.
13. Polim-Agri, www.poliagri.com.br accessed in January 2013.
14. Thomas, D. S.; Heagney, G.A.; *Aust. For.* **2011**, *74*, 133.
15. Agaba, H.; Orikiriza, L. J. B.; Esegu, J. F. O; Obua, J.; Kabasa, J. D.; Huettermann, A.; *Clean-Soil Air Water* **2010**, *38*, 328.
16. Garcia, A. L. A.; Padilha, L.; Garcia, A. W. R.; Mendes, A. N. G.; Carvalho, C. H. S.; *Coffee Sci.* **2011**, *6*, 1.
17. Neves L. N. C. G.; Pinto, L. E. V.; Marques, T. A., Benincasa, F.; Sedano, M. V.; Rampazo, E. M.; Santos, A. T.; Deltrejo Jr., E. L.; Markndorf, P. L.; Godinho, A. M. M.; *Colloquium Agrariae* **2010**, *6*, 2.
18. Gender, M. B.; *Int. J. Toxicol*. **2005**, *24*, suppl 2, 21.
19. www.accepta.com/images/product-safety-data/MSDS_Accepta%20Ltd_ Accepta%204363.pdf accessed in January 2013.
20. Qin, S.; Wu, Z.; Rasool, A.; Li, C.; *J. Appl. Polym. Sci.* **2012**, *126*, 1687.
21. Cândido, J. S.; Leitão, R. C. F.; Ricardo, N. M. P. S.; Feitosa, J. P. A.; Muniz, E. C.; Rodrigues, F. H. A.; *J. Appl. Polym. Sci.* **2012**, *123*, 879.
22. Zhang, L.; Luo, Z.; Zhou, A.; Yang J.; Yan, L.; *CN pat. 102,093,900-A*, **2011**
23. Inotec Glienke&Glienke GBR; *DE pat. 202,011,003,679-U1*, **2011**.
24. Lin, J.; Wu, J.; Yang, Z.; Pu, M.; *Macromol. Rapid Comm.* **2001**, *22*, 422.
25. Sirousazar, M.; Kokabi, M.; Hassan, Z. M.; Bahramian, A. R.; *J. Appl. Polym. Sci.* **2012**, *125*, E122.
26. Aalaie, J.; Youssefi, M.; *J. Macromol. Sci., Part B: Phys.* **2012**, *51*, 1027.
27. Bulut, Y.; Akcay, G.; Elma, D.; Serhath, I. E.; *J. Hazard. Mater*. **2009**, *171*, 717.
28. Wang, W. B.; Zheng, Y. A.; Wang, A. Q.; *Polym. Adv. Technol.* **2008**, *19*, 1852.
29. Qi, X.; Liu, M.; Chen, Z.; Liang, R.; *Polym. Adv. Technol.* **2007**, *18*, 184.
30. Zhang, J.; Wang, A.; *React. Funct. Polym.* **2007**, *67*, 737.
31. Bardajee, G. R.; Pourjavadi, A.; Soleyman, R.; Ghavami, S.; *Adv. Polym. Technol*. **2012**, *31*, 41.
32. Li, A. Wang, A. Q.; *Eur. Polym. J.* **2005**, *41*, 1630.
33. Santos, P. S.; *Ciência e Tecnologia das Argilas*, vol. 1, 2ª ed.; Edgard Blucher Ltda: São Paulo, Brasil, 1989.
34. Deer, W. A.; Howie, R. A.; Zussman, J.; *Minerais Constituintes das Rochas: Uma Introdução*; Fundação Calouste Gulbenkian: Portugal, 2000.
35. (a) http://s3.amazonaws.com/magoo/ABAAABgWYAK-1.png; (b) http://accessscience.com/search.aspx?SearchInputText=Dolomite&ucTopSearch %24ContentTypeSelect=all accessed in January, 2013.
36. Jeon, C. H.; Makhaeva, E. E.; Khokhlov, A. R.; *Macromol. Chem. Phys*. **1998**, *199*, 2665.
37. Okay, O., Yilmaz, Y.; Kaya, D. Keskinel, M.; Pekcan, O.; *Polym. Bull.* **1999**, *43*, 425.
38. Magalhães, A. S. G.; Almeida Neto, M. P.; Bezerra, M. N.; Ricardo, N. M. P. S.; Feitosa, J. P. A.; *Quim. Nova*, **2012**, *35*, 1464.
39. Guilherme, M. R.; Reis, A. V.; Takahashi, S. H.; Rubira, A. F.; Feitosa, J. P. A.; Muniz, E. C.; *Carbohydr. Polym.* **2005**, *61*, 464.
40. Rippel, M. M.; Galembeck, F.; *BR pat. PI 1002.509-0 A2*, deposited on July 08, **2010**.
41. Liu, X.; Hu, M; Hu, Y.; *J. Centr. South Univ. Technol.* **2008**, *15*, 193.
42. Yao, K. J.; Zhou, W. J.; *J. Appl. Polym. Sci*. **1994**, *53*, 1533.
43. Ray, S. S.; Okamoto, M.; *Prog. Polym. Sci*. **2003**, *28*, 1539.
44. Kiatkamjornwong, S.; Wongwatthanasatien, R.; *Macromol. Symp.* **2004**, *207*, 229.
45. Silverstein, R. M.; Webster, F. X.; *Spectrometric Identification of Organic Compounds*, 6th ed.; Wiley: New York, USA, 1998.
46. Molu, Z. B.; Seki, Y.; Yurdakoc, K.; *Polym. Bull.* **2010**, *64*, 171.
47. Santillán, J.; Williams, Q.; *Phys. Earth Planet. Inter.* **2004**, *143*, 291.

Submitted: October 20, 2012
Published online: February 26, 2013